

## Scanning Beam Interference Lithography

Paul T. Konkola<sup>1</sup>, Carl G. Chen, Ralf K. Heilmann, G.S. Pati, and Mark L. Schattenburg  
Massachusetts Institute of Technology, Cambridge, MA 02139

### 1 Introduction

We are developing a system for patterning large-area, nanometer-accuracy gratings that are appropriate for semiconductor metrology [1]. Our system, termed Scanning Beam Interference Lithography (SBIL), uses the interference fringes between two coherent laser beams to define highly coherent gratings in photoresist. The substrate is step-and-scanned under the interference pattern to produce large gratings.

The ultimate goal of the SBIL system is to write gratings and grids with sub-nanometer distortions over substrates up to 300 mm in diameter. These ultra-low distortion gratings would enable important advances in metrology, electro-optics, spectroscopy, and many other applications.

Figure 1 depicts the SBIL concept. The optics closely resemble those of the traditional interference lithography system [2, 3] but the image is much smaller than the total desired patterning area. The grating image diameter is typically designed to be between 200  $\mu\text{m}$  and 2 mm. Large gratings are fabricated by scanning the substrate at a constant velocity under the image. At the end of the scan the stage steps over by an integer number of grating periods and reverses direction for a new scan. The interference pattern has a Gaussian intensity envelope since we interfere Gaussian beams. A maximum step size is constrained by the desired dose uniformity. For instance, a step size of 0.9 times the Gaussian beam  $1/e^2$ -radius produces dose uniformity of better than 1%.

The system has the significant added problem over previous interference lithography systems of accurately synchronizing the interference image to the moving substrate. Therefore, the design includes correction for stage error and the lithography interferometer's phase error by feedback to a high bandwidth fringe locking controller.

The optical design incorporates means for spatial filtering and adjustment of intensity, polarization, wavefront curvature, and spot size. The nominal period,  $\Lambda$ , of the interference fringes is controlled by the beam incident angle  $\theta$  and is given by

$$\Lambda = \frac{\lambda}{2 \sin \theta}. \quad (1)$$

Here  $\lambda$  is the wavelength of the laser.

The relatively small beams used in SBIL provide a major benefit in ease of obtaining small wavefront distortions [4]. Furthermore, by scanning the image, distortions along the scan direction can be averaged out. The overlap of scans provides even further averaging of the wavefront distortions. Also, critical alignments such as lens positioning and angle of interference are much relaxed for the small beams.

In our approach, we aim to demonstrate nanometer-level repeatable grating writing first. Then, self-calibration methods [5] will be implemented to correct systematic errors and achieve nanometer-level accuracy. We are designing and implementing a system with a CW 351.1 nm wavelength argon-ion laser that

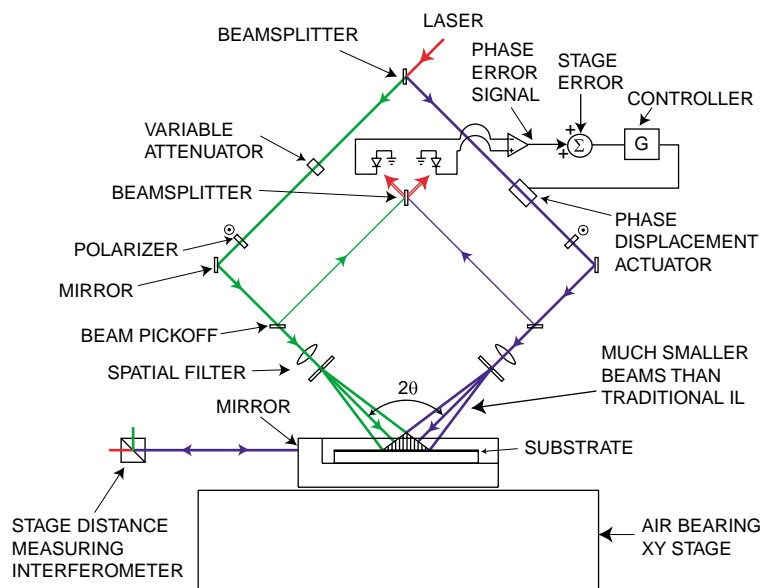


Figure 1: SBIL system concept

<sup>1</sup>email: konkola@mit.edu.

is intended to achieve nanometer level distortions for arbitrarily selected grating periods in the range of 200 nm to 2  $\mu\text{m}$ . Realizing our performance goals is a major challenge because of the many error sources in lithography. We elaborate on the major error sources in the next section.

## 2 System Errors

There are many sources of errors in our system. We break them down into six categories: stage interferometer, fringe locking, metrology frame, substrate frame, period control, and image distortion.

Figure 2 illustrates definitions of error coordinate systems. The distance,  $x_d$  is the displacement between the stage and column reference mirrors. We define errors in this measurement as stage interferometer errors. The distance  $x_f$  is the displacement of the fringe pattern at the substrate-interference image interface relative to the column reference. During writing, we shift the fringes with a high speed acousto-optic fringe locking system [6] such that

$$x_d - x_f + x_o = N M \Lambda. \quad (2)$$

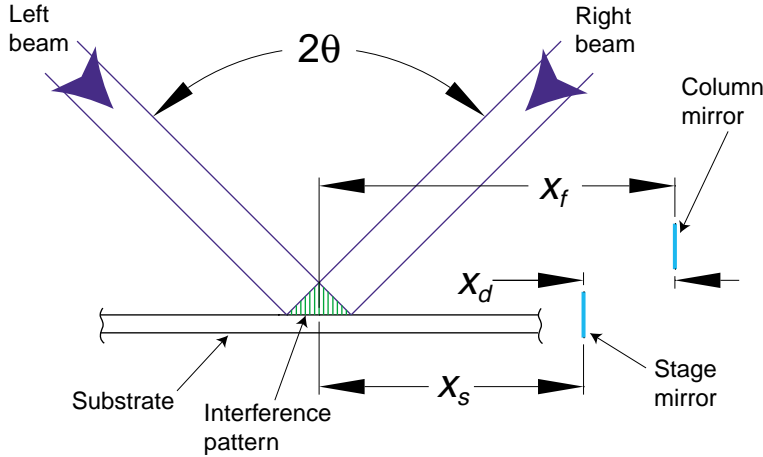


Figure 2: Definition of coordinate systems for error terms.

Here  $x_o$  is a constant depending on the location of the first scan and  $N$  is the integer scan number incremented from zero. The distance  $M\Lambda$  is the step size between scans, where  $M$  is an integer and  $\Lambda$  is the period of the interference image.

Inaccuracy in the fringe position,  $x_f$ , comprises two error categories. The first is the fringe locking error, which is due to inaccuracy in the fringe locking sensor signal and the controller's inability to lock out the total fringe locking error signal. Inaccuracy in the fringe locking sensor signal is due to air index variations and electronic inaccuracy. The metrology frame error category contains the remaining sources of errors in  $x_f$ .

These errors are due to the non-collocation of the sensor with the fringes on the wafer, alignment errors, and disturbance of the sensor optics with respect to the column reference.

The position of a substrate location relative to the stage mirror is  $x_s$ . Inaccuracy in this position is the substrate frame error; during writing the substrate must accurately track the stage mirror for this error to be zero. Furthermore, the substrate must be clamped during writing in substantially the same way that it will be used as a metrology reference, otherwise clamping distortions will limit the accuracy of the reference.

Another category of error is period control. Variations in  $\lambda$  and interference angle,  $\theta$ , limit the period control. For 1 nm of accumulated phase error across a 1 mm image radius we must control the period to 1 ppm [3].

The image distortion category is due to nonlinearity of the interference image. To some extent, the image nonlinearity can be averaged out by tightly overlapping adjacent scans but this approach limits throughput and image contrast is sacrificed. Therefore, we are trying to achieve image linearity on the same order as for the other error categories.

### 3 System Design

Our accuracy goal requires fringe locking to the substrate with nanometer-level spatial phase errors while controlling the fringe period to approximately one part per million. Furthermore, our system design faces severe requirements on the design of the substrate and metrology frames, stage and vibration controls, environmental controls, displacement interferometry, lithography interferometer phase locking, planarity of the interfering waves, and control of the fringe period. We review how our design, shown in Figure 3, addresses some of these error categories.

The system employs an X-Y air bearing stage, four axes of column referencing heterodyne laser interferometry, beam alignment systems [7], period measurement system [3], image distortion measurement system, acousto-optic fringe locking [6], environmental controls, active and passive vibration isolation with feed-forward, and beam steering [8].

We require a length scale repeatable to  $\pm 1$  nm/.150 m or  $\pm 7$  ppb to ensure that we can repeatably write gratings. Moreover, the index of air and laser vacuum wavelength are unstable and we must have an accurate way to scale the phase readings from our heterodyne electronics. A grating length-scale reference is included on the chuck to calibrate the wavelength of the stage interferometer. Our system is designed to read the phase of a grating that is nominally the same period that we are setup to write [6]. This scale calibration method replaces air-index calculations that may have experimental uncertainties of  $\pm 30$  ppb [9]. Furthermore, the grating length scale allows us to use a commercial heterodyne laser in place of a less convenient but highly wavelength-stable iodine-stabilized laser system. We continuously take measurements from our refractometer once we establish our length scale from the grating reference. Thus, in real-time we can correct for the wavelength change of the stage interferometer. The writing interferometer uses an achromatic grating-based interferometer configuration where the image period is insensitive to air index changes and vacuum wavelength instability of the UV laser.

Our system's repeatability is determined by reading the phase of a previously exposed substrate. This direct measurement of the grating phase allows us to assess the repeatability of the stage's displacement interferometer. We present measurements from our stage and grating-based interferometers .

### 4 Conclusions

Our accuracy goal requires fringe locking to the substrate with nanometer-level spatial phase errors while controlling the fringe period to approximately one part per million. We have designed and are in an evolutionary process of implementing a SBIL system for producing gratings with repeatability of a few nanometers.

We are in the process of major upgrades to our system. We are incorporating thermally stable and higher resonant frequency metrology frames. Also, an environmental enclosure is being installed to control temperature ( $\pm 0.005$  °K), relative humidity ( $< \pm 0.8\%$ ), and pressure gradient ( $< 15.5$  Pa/m). Acoustic suppression is also a necessary feature of the enclosure in our noisy lab [6]. We will present the latest repeatability results in grating reading, writing, and stage interferometry.

### References

- [1] M. Schattenburg *et al.*, J. Vac. Sci. Technol. B **17**, 2692 (1999).
- [2] J. Ferrera, PhD dissertation, Massachusetts Institute of Technology, Department of Electrical Engineering and Computer Science, 2000.
- [3] C. G. Chen *et al.*, to be published in J. Vac. Sci. Technol. B (2001).
- [4] C. G. Chen, Master's thesis, Massachusetts Institute of Technology, Department of Electrical Engineering and Computer Science, 2000.
- [5] C. J. Evans, R. J. Hocken, and W. T. Estler, CIRP Annals **45**, 617 (1996).

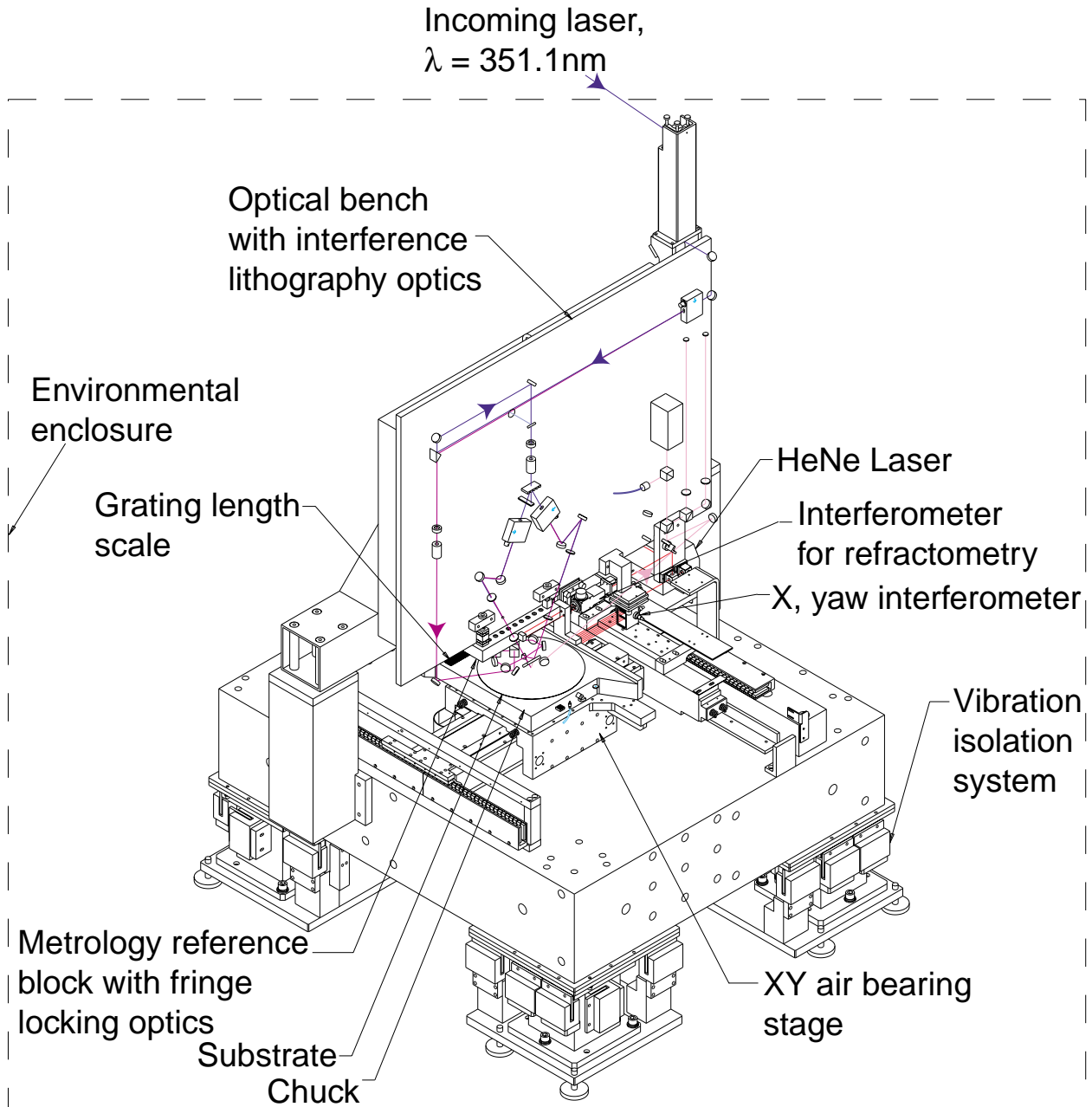


Figure 3: SBIL design showing optics and some subsystems. Details such as optical mounts, fasteners, and holes may not be shown.

[6] R. K. Heilmann *et al.*, to be published in *J. Vac. Sci. Technol. B* (2001).

[7] C. G. Chen *et al.*, submitted to these proceedings (2001).

[8] P. Konkola, C. G. Chen, R. Heilmann, and M. L. Schattenburg, *J. Vac. Sci. Technol. B* **18**, 3282 (2000).

[9] K. P. Birch and M. J. Downs, *Metrologia* **31**, 315 (1994).